Robotica (2008) volume 26, pp. 703–710. © 2008 Cambridge University Press
doi:10.1017/S026357470800430X Printed in the United Kingdom

Force/position control self-tuned to unknown surface slopes using motion variables

Zoe Doulgeri* and Yiannis Karayiannidis

Department of Electrical and Computer Engneering, Aristotle University of Thessaloniki, Thessaloniki 54124, Greece

(Received in Final Form: February 7, 2008. First published online: March 20, 2008)

SUMMARY

This work considers the problem of force/position regulation for a robotic finger in compliant contact with an unknown curved surface resulting in uncertain force and position control subspaces. The proposed controller is an adaptive control scheme of a simple structure that achieves the desired target by the on-line tuning of the position and force control actions to their corresponding actual subspaces at the desired point using motion state feedback. The local asymptotic stability of the system equilibrium point is proved and an estimate of the region of attraction is given. The controller performance is illustrated by a simulation example.

1. Introduction

Kinematic uncertainties arise in many robotic contact tasks due to the lack of knowledge about the geometry and the position of the contacted surface. In such tasks the control space is naturally divided into two complementary subspaces for the position and force control that cannot be accurately specified for an unknown surface. Hence surface kinematic uncertainties affect the control target as opposed to dynamic uncertainties that mainly affect the system knowledge. Another class of kinematic uncertainties refer to robot kinematic parameters like robot link lengths that affect the robot Jacobian as well as the robot dynamic terms.

One way to reduce the surface uncertainty is to use an off-line procedure for the identification of the surface to be contacted and in turn employ a position/force controller that has been proved to achieve the task for a known surface[1,2]. The identification procedure can be based on optical sensor measurements as well as preliminary exploration of the surface by the robot tip using force and tactile measurements. This solution may be acceptable if the environment with which the robot interacts does not dynamically change and an immediate task completion is not required; in the opposite case an on-line solution should be sought. This solution should identify on-line the actual force and position subspaces in order to achieve the actual control target. Uncertainties either structural or parametric that may be substantial call for adaptive control techniques that are able to achieve the control target despite their presence. However, adaptive control techniques that do not result in uncertain parameter identification cannot achieve the actual control target, in an uncertain target case, as it is the case of position/force control on an unknown surface.

In the case of constrained motion, on-line surface identification using force, velocity measurements and vision feedback has been extensively used relying on the fact that tip velocities belong to the tangent space while force measurements in the absence of friction belong to the normal space[3–7]. However, those works that use adaptive control laws[3,4,7] are based on the assumption of known surface geometrical model structure (circle, ellipse, etc.) although in practice, ideal geometrical models rarely reflect a real surface and model structural uncertainties may be present.

In the case of a compliant contact with friction that is, for example, typical in dexterous manipulation of unknown objects by soft robotic fingertips, the deformation kinematics imply the existence of non-negligible velocities along the surface normal direction. As a result, on-line surface slope identification methods that are used for the constrained case cannot be applied. When the friction is assumed to be negligible, measurements by force/torque sensors can be utilized to obtain the normal direction[8]. However, there are considerable friction forces particularly when there is an area contact. In the presence of friction, an experimental work is presented combining visual servoing and direct force control[9]. There have also been proposed controllers[10,11] that achieve force regulation and position errors, dependent on the surface orientation estimate error. Recently, the actual control target has been achieved by an adaptive control law proposed by the authors[12], but the analysis holds only for flat surfaces.

In this work, the general case of an unknown curved surface is considered. A simple control law without the use of force measurements is proposed that achieves the actual force/position regulation target despite surface kinematic uncertainties. Any knowledge and assumption regarding the surface geometrical model is not required. The controller achieves the task by the on-line tuning of the position and force control actions to their corresponding actual subspaces at the desired point.

2. Model Description

2.1. System kinematics

Consider a robot finger with soft hemispherical fingertip of radius r in contact with a rigid surface S. Let $q \in \Re^{n_q}$ be the vector of the generalized joint variables and $\{B\}$ the inertia frame attached at the finger base (Fig. 1). Consider

* Corresponding author. E-mail: doulgeri@eng.auth.gr

https://doi.org/10.1017/S026357470800430X Published online by Cambridge University Press

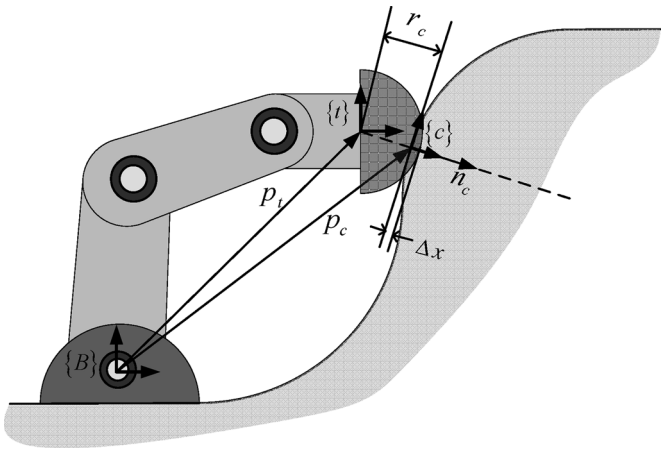


Fig. 1. A robot finger with a soft hemispherical fingertip in contact with a curved surface.

also the frame $\{t\}$ at the finger rigid tip with position $p_t \in \Re^3$ and orientation R_t that can be parameterized by three angles $\phi_t \in \Re^3$ around the axes of the inertia frame. Let the generalized rigid tip position be $p = [p_t^T \ \ \phi_t^T]^T \in \Re^6$. The generalized velocity $\dot{p} = [\dot{p}_t^T \ \ \omega_t^T]^T \in \Re^6$, where $\omega_t = \dot{\phi}_t$, is related to the joint velocity $\dot{q}$ through the rigid tip Jacobian $J = [J_v^T \ \ J_\omega^T]^T \in \Re^{6\times n_q}$ as follows:

$$\dot{p} = J(q)\dot{q}. \tag{1}$$

At the center point of the contact area, we attach the contact frame $\{c\}$, described by the position vector p_c and the orientation matrix $R_c = [n_c \ \ o_c \ \ a_c]$, such that $n_c \in \Re^3$ is the unit vector normal to the contact surface pointing inwards. In the case of a flat surface n_c is constant.

Note that when the finger is in contact with the surface the rigid tip position can be expressed as follows:

$$p_t = p_c - n_c r_c, \tag{2}$$

where $r_c = r - \Delta x$ is the fingertip deformable radius. By projecting (2) on the surface tangent at the contact point with the projection matrix $Q_c = I - n_c n_c^T$ we can find that the contact point identifies with the rigid tip projection on the surface i.e., $Q_c p_c = Q_c p_t$. Moreover, we can derive the material deformation as a function of p_c, p_t:

$$\Delta x = r - n_c^T(p_c - p_t). \tag{3}$$

It can be easily proved that its derivative depends only on the normal to the surface rigid tip velocity:

$$\Delta\dot{x} = n_c^T \dot{p}_t. \tag{4}$$

2.2. Contact force model

As the fingertip presses upon the surface, the soft hemispherical tip deforms forming a contact area and giving rise to a reaction force. We assume that stresses of the deformed fingertip are symmetrically distributed over the contact area and hence the aggregated force arises at the center of the contact area at a direction normal to the surface. This force can be expressed as $F_c = n_c f$, where the force magnitude

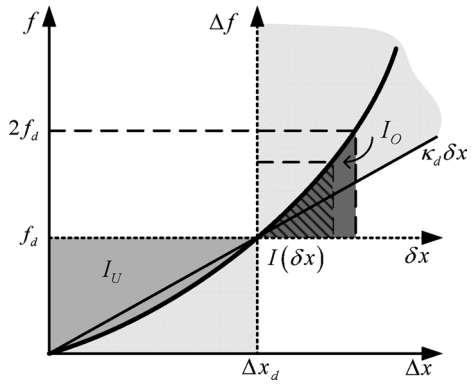


Fig. 2. Normal contact force model.

f is in general a monotonically increasing, continuously differentiable non-linear function of Δx: $f(\Delta x)$ if $\Delta x > 0$, $f = 0$ if $\Delta x \le 0$. The contact force F_c is mapped to the rigid tip as a generalized force $F = nf \in \Re^6$, with $n = [\, n_c^T \ \ 0_3^T]^T \in \Re^6$ denoting the generalized normal direction.

Let us define the force error $\Delta f = f - f_d$ where f_d is the desired force magnitude, the corresponding deformation error $\delta x = \Delta x - \Delta x_d$ where $\Delta x_d = f^{-1}(f_d)$ and the potential energy due to deformation error $I(\delta x) = \int_{\Delta x_d}^{\delta x + \Delta x_d} (f(\xi) - f_d)d\xi > 0$, for $\delta x \neq 0$ (Fig. 2). Function Δf belongs to the sector $[\kappa_d, +\infty)$, where κ_d is a positive constant, i.e., $\Delta f \delta x \ge \kappa_d \delta x^2$. Hence it can be easily proved that:

$$I(\delta x) \ge \frac{\kappa_d}{2}\delta x^2. \tag{5}$$

Moreover, dynamic friction forces may arise during the motion of the end-effector along the motion directions that are complement to the surface generalized normal. Several models have been proposed for dynamic frictional forces. Here, we assume that frictional forces are dependent on the end-effector velocities such that:

$$F_s = \begin{bmatrix} \xi_p(\|\dot{p}\|)Q_c\dot{p}_t \\ \xi_\phi(\|\dot{p}\|)\omega_t \end{bmatrix}.$$

where $\xi_p(\|\dot{p}\|)$, $\xi_\phi(\|\dot{p}\|)$ are scalar positive coefficients with $\xi_p(\|\dot{p}\|)$, $\xi_\phi(\|\dot{p}\|) \le \tilde{\xi}\|\dot{p}\|$ where $\tilde{\xi}$ is a positive constant.

2.3. Robot dynamic model

The dynamic model of the robot in contact with the surface can be written as follows:

$$M(q)\ddot{q} + \left(\frac{1}{2}\dot{M}(q) + S(q,\dot{q})\right)\dot{q} + g(q) + J^T(q)\begin{bmatrix} \xi_p(\|\dot{p}\|)Q_c\dot{p}_t \\ \xi_\phi(\|\dot{p}\|)\omega_t \end{bmatrix} + J^T(q)nf = u \tag{6}$$

where $M(q) \in \Re^{n_q\times n_q}$ is the robot inertia matrix that is positive definite, $S(q,\dot{q}) \in \Re^{n_q\times n_q}$ is a skew symmetric matrix, $g(q) \in \Re^{n_q}$ denotes the gravity vector and u denotes the input control law.

https://doi.org/10.1017/S026357470800430X Published online by Cambridge University Press

3. Control Law and Surface Kinematic Uncertainties

When the contacted environment is kinematically uncertain, the desired position target cannot be exactly determined. Instead, we can use a commanded position based on an initial estimate that can be in reality inside or outside the actual surface and let the controller drive the contact point on the projection of the commanded position on the surface. Furthermore, in the case of a soft robotic fingertip the contact position p_c cannot be accurately calculated or measured. Instead, the position control loop can be designed around the rigid tip position p_t that corresponds to a unique p_c, and can be calculated given measurements of the joint positions and knowledge of rigid tip kinematics. Rigid tip kinematics can be considered known in robotic fingers as opposed to the cases of robots holding a tool of unknown length or uncertain position.

Let p_{td} be the commanded rigid tip position that corresponds to a unique p_{cd} on the actual surface. Let $n_{cd} = n_c(p_{td})$ be the actual unit vector normal to the surface at the desired position along which it is desired to apply a force of f_d magnitude. Then, the position regulation target is to achieve the desired position on the surface i.e., $Q_{cd}\Delta p_t = 0$ with $Q_{cd} = I - n_{cd}n_{cd}^T$ or equivalently to minimize the position error $\Delta p_t = p_t - p_{td}$.

This controller objective corresponds to a unique rigid tip position noted by

$$p_{td}^* = Q_{cd}p_{td} + n_{cd}\left(n_{cd}^T p_{cd} - r_{cd}\right), \tag{7}$$

where $r_{cd} = r - \Delta x_d$ with Δx_d being the desired fingertip deformation. The rigid tip position p_{td}^* is generally unknown under uncertainties in material compliance and surface kinematics. Hence, the position error $\bar{p}_t = p_t - p_{td}^*$ that is zero at equilibrium cannot be used for control purposes. Instead Δp_t is used that is minimized when the control target is achieved and the two errors are related as follows (Fig. 3):

$$\Delta p_t = \bar{p}_t - n_{cd}(r_{cd} + d) \tag{8}$$

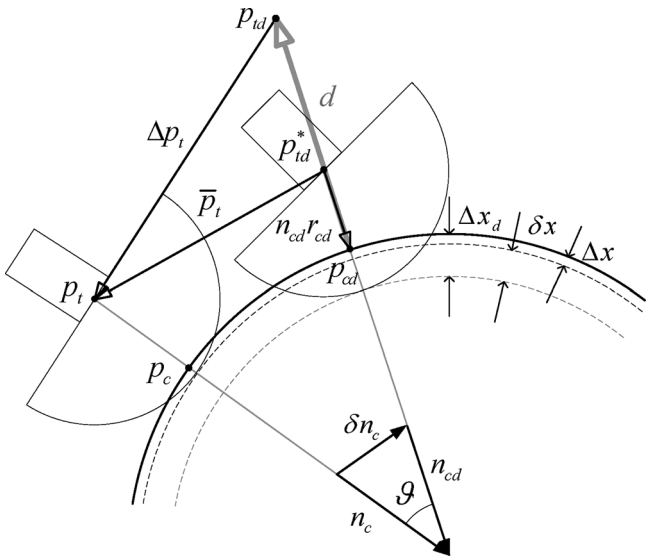


Fig. 3. Task description in the planar case.

where $d = n_{cd}^T(p_{td} - p_{cd})$ is the distance between the desired contact point and the commanded rigid tip position, and hence it is indicative of the initial error of the estimate regarding the contacted surface position and orientation (Fig. 3). Let us assume that there is a unique position p_c on the curved surface for which $Q_{cd}\Delta p_t = 0$; this assumption excludes cases of curved surfaces having reachable (by the robot) points of antipodal orientations. Under this assumption there exist positive constants c_n, c_p so that the difference between the current normal vector and the normal vector at the desired position $\delta n_c = n_c - n_{cd}$ (Fig. 3) as well as the difference between the current and the desired contact point along the surface normal at the desired position $n_{cd}^T(p_c - p_{cd})$ can be upper bounded as follows:

$$\|\delta n_c\| \le c_n \|Q_{cd}\Delta p_t\| \tag{9}$$

$$\left|n_{cd}^T(p_c - p_{cd})\right| \le c_p \|Q_{cd}\Delta p_t\|. \tag{10}$$

If ϑ is the angle formed by n_c and n_{cd} on their common plane (Fig. 3) with $\cos\vartheta = n_c^T n_{cd}$, then for the case of a flat surface $\cos\vartheta = 1, \delta n_c = 0$ and $n_{cd}^T p_c = n_{cd}^T p_{cd}$. Inequalities (9) and (10) will be used in the stability analysis.

We can now propose the following input control law with on-line gravity compensation in order to achieve force, position regulation as well as identification of the desired normal direction:

$$u = J^T\left(\hat{n}_d(t)f_d - k_v\dot{p} - \begin{bmatrix}\alpha k_v \hat{Q}_{cd}(t)\Delta p_t \\ k_\phi e_\phi\end{bmatrix}\right) + g(q), \tag{11}$$

where α, k_v, k_ϕ are positive control gains, $e_\phi = \phi_t - \phi_{td}$ is the rigid tip orientation error and $\hat{n}_d(t) = [\ \hat{n}_{cd}^T(t)\ \ 0_3^T\ ]^T$ where $\hat{n}_{cd}$, $\hat{Q}_{cd}(t)$ are on-line estimates of the normal vector at the desired position and its orthogonal space projector; hence $\hat{Q}_{cd}(t)\hat{n}_{cd}(t) = 0$. The normal vector estimate $\hat{n}_{cd}(t)$ is updated by the following law:

$$\dot{\hat{n}}_{cd}(t) = -\gamma\,\hat{Q}_{cd}(t)(\dot{p}_t + \alpha\Delta p_t), \tag{12}$$

where γ, α are positive control gains that affect the update rate and the importance of the position error Δp_t in the adaptive law, respectively. The normal vector estimates can be in general non-unit but the adaptive law (12) ensures the invariance of the normal vector norm since

$$\frac{d(\hat{n}_{cd}^T\hat{n}_{cd})}{dt} = 0.$$

Hence, given an initial estimate of $\|\hat{n}_{cd}(0)\| = 1$ the updated vector $\hat{n}_{cd} = \hat{n}_{cd}(t)$ preserves its unit norm and the projection matrix is given by $\hat{Q}_{cd}(t) = I - \hat{n}_{cd}(t)\hat{n}_{cd}^T(t)$.

Notice that the controller fully compensates for the gravity torque. The implied assumption is that the dynamic parameters involved in the robot gravity term i.e., masses, mass centers as well as lengths of the rigid links are known or have been identified in advance. Gravity parameter uncertainties mainly affect robots having uncertain end-effector dynamics when holding objects or tools rather than robotic fingers. Further, notice that the position controller

https://doi.org/10.1017/S026357470800430X Published online by Cambridge University Press

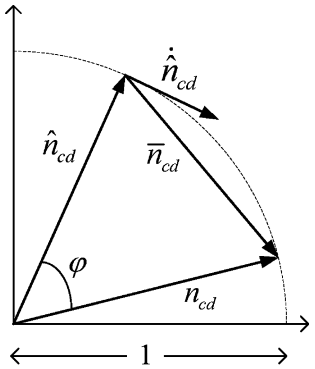


Fig. 4. Normal vector estimation in the planar case.

requires feedback of quantities $\dot{p} = [\ \dot{p}_t^T \quad \omega_t^T\ ]^T, \Delta p_t, e_\phi$ that can be calculated from the robot kinematics while closing the force control loop is not needed for proving convergence to the desired force. However, if a force sensor is available a proportional force control term can, e.g., be added to improve the dynamics of the force response.

Let us further define the estimate errors $\bar{n}_{cd} = n_{cd} - \hat{n}_{cd}$ and $\bar{Q}_{cd} = Q_{cd} - \hat{Q}_{cd}$, that is a symmetric matrix. These errors can be related to the angle $\varphi = \varphi(t)$ formed by vectors $n_{cd}, \hat{n}_{cd}$ on their common plane (Fig. 4)

$$\|\bar{n}_{cd}\| = \sqrt{2}\sqrt{1-\cos\varphi} \tag{13}$$

$$\|\bar{Q}_{cd}\| = |\sin\varphi|, \tag{14}$$

where $\cos\varphi = n_{cd}^T \hat{n}_{cd}$ and $\|\cdot\|$ denotes the Euclidean norm of a vector and the spectral norm of a matrix. Moreover, using (13) and (14) it can be shown that:

$$\|\bar{Q}_{cd}\| = \psi\|\bar{n}_{cd}\| \quad \text{with} \quad \psi = \sqrt{\frac{1+\cos\varphi}{2}} < 1 \tag{15}$$

$$\left|n_{cd}^T \bar{n}_{cd}\right| = \left|\hat{n}_{cd}^T \bar{n}_{cd}\right| = |1-\cos\varphi| = \frac{\|\bar{n}_{cd}\|^2}{2}. \tag{16}$$

4. Stability Analysis

Substituting the control law (11) in system model (6), adding and subtracting nf_d we obtain the closed loop system:

$$M\ddot{q} + \left(\frac{1}{2}\dot{M} + S\right)\dot{q} + J^T \begin{bmatrix} \xi_p(\|\dot{p}\|) Q_c \dot{p}_t \\ \xi_\phi(\|\dot{p}\|)\omega_t \end{bmatrix} + k_v J^T \dot{p} + J^T \begin{bmatrix} \alpha k_v \hat{Q}_{cd} \Delta p_t \\ k_\phi e_\phi \end{bmatrix} + J^T(n\Delta f + f_d \bar{n}_d + \delta n f_d) = 0, \tag{17}$$

where $\bar{n}_d = [\ \bar{n}_{cd}^T \quad 0_3^T\ ]^T$ is the generalized estimate error and $\delta n = [\ \delta n_c^T \quad 0_3^T\ ]^T$.

We can write the inner product of (17) with the vector $s = \dot{q} + J^{-1}(\alpha e_p + \beta \bar{n}_d)$, where $e_p = [(Q_{cd}\Delta p_t)^T \quad 0_3^T\ ]^T$ and β a positive constant, as follows:

$$\frac{dV}{dt} + W = 0, \tag{18}$$

where

$$V = \frac{1}{2}\dot{p}^T M_p \dot{p} + \beta \bar{n}_d^T M_p \dot{p} + \frac{(k_v\beta + f_d)}{2\gamma}\|\bar{n}_d\|^2 + I(\delta x) + \alpha k_v \|e_p\|^2 + \alpha e_p^T M_p \dot{p} + \frac{1}{2}k_\phi \|e_\phi\|^2 \tag{19}$$

with $M_p = J^{-T} M J^{-1}$ as the positive definite inertia matrix expressed in the rigid tip space, and

$$\begin{aligned} W = {} & k_v\|\dot{p}\|^2 + \xi_p(\|\dot{p}\|)\dot{p}_t^T Q_c \dot{p}_t + \xi_\phi(\|\dot{p}\|)\omega_t^T \omega_t \\ & + \beta f_d \|\bar{n}_d\|^2 + \alpha^2 k_v \|e_p\|^2 - \dot{p}^T(\beta\gamma \hat{Q}_d + \alpha Q_d) M_p \dot{p} \\ & - (\alpha e_p + \beta \bar{n}_d)^T Z(q,\dot{q})\dot{p} + \xi_p(\|\dot{p}\|)(\alpha Q_{cd}\Delta p_t \\ & + \beta \bar{n}_{cd})^T \dot{p}_t + \alpha\beta\gamma\, \dot{p}^T M_p \bar{Q}_d \Delta p - \alpha^2 k_v e_p^T \bar{Q}_d \Delta p \\ & + \alpha f_d \bar{n}_d^T \bar{Q}_d \Delta p_t - \alpha k_v \dot{p}^T \bar{Q}_d \Delta p - \alpha\beta\gamma e_p^T M_p \dot{p} \\ & + (\alpha f e_p + \beta f \bar{n}_d + f_d \dot{p})^T \delta n + (\beta k_v + f_d)\bar{n}_d^T \hat{n}_d \hat{n}_d^T \dot{p} \\ & + \beta \bar{n}_d^T n_d \Delta f \end{aligned} \tag{20}$$

where $Q_d = \mathrm{diag}_{\mathrm{block}}[Q_{cd} \quad O_3]$, $\hat{Q}_d = \mathrm{diag}_{\mathrm{block}}[\hat{Q}_{cd} \quad O_3]$, $\bar{Q}_d = Q_d - \hat{Q}_d$, $\Delta p = [\Delta p_t^T \quad e_\phi^T]^T$ and $Z(q,\dot{q}) = \dot{J}^{-T} M + J^{-T}(\frac{1}{2}\dot{M} - S)J^{-1}$. Note that the term $Z(q,\dot{q})\dot{p}$ is quadratic with respect to the rigid tip generalized velocities with bounded coefficients. Hence, there exists a positive constant c, such that:

$$\|Z(q,\dot{q})\dot{p}\| \le c\|\dot{p}\|^2 \tag{21}$$

Proposition 1. *Function V defined in (19) is positive definite with respect to $\dot{p}$, δx, $Q_c\Delta p_t$, e_ϕ, $\bar{n}_{cd}$ provided that the following condition holds:*

$$k_v > 2\lambda_M \max(\alpha, \beta\gamma) \tag{22}$$

where λ_M is the maximum eigenvalue of the inertia matrix M_p.

Proof: Note that:

$$\begin{aligned} & \frac{1}{4}\dot{p}^T M_p \dot{p} + \beta \bar{n}_d^T M_p \dot{p} \\ & = \frac{1}{4}(\dot{p} + 2\beta\bar{n}_d)^T M_p (\dot{p} + 2\beta\bar{n}_d) - \beta^2 \bar{n}_d^T M_p \bar{n}_d \\ & \ge -\beta^2 \lambda_M \|\bar{n}_{cd}\|^2 \end{aligned} \tag{23}$$

and

$$\begin{aligned} & \frac{1}{8}\dot{p}^T M_p \dot{p} + \alpha e_p^T M_p \dot{p} \\ & = \frac{1}{8}(\dot{p} + 4\alpha e_p)^T M_p (\dot{p} + 4\alpha e_p) - 2\alpha^2 e_p^T M e_p \\ & \ge -2\alpha^2 \lambda_M \|Q_{cd}\Delta p_t\|^2. \end{aligned} \tag{24}$$

https://doi.org/10.1017/S026357470800430X Published online by Cambridge University Press

Using (23) and (24), V is lower bounded, i.e.,

$$V \geq \frac{1}{8}\dot{p}^T M_p \dot{p} + \frac{\beta}{2\gamma}(k_v - 2\beta\gamma\lambda_M)\|\bar{n}_{cd}\|^2 + \frac{f_d}{2\gamma}\|\bar{n}_{cd}\|^2 + \alpha(k_v - 2\alpha\lambda_M)\|Q_{cd}\Delta p_t\|^2 + I(\delta x) + \tfrac{1}{2}k_\phi\|e_\phi\|^2 \quad (25)$$

and positive definite if $k_v > 2\lambda_M \max(\alpha, \beta\gamma)$. □

Proposition 2. *There exists a constant $\beta > 0$ for which function W given by (20) is positive definite with respect to $\dot{p}$, $\bar{n}_{cd}$, $Q_{cd}\Delta p_t$ in a region of the system state dependent on the control gains.*

Proof: Using (21) and $\xi_p \leq \tilde{\xi}\|\dot{p}\|$ the terms of the second line of (20) are quadratic with respect to the end-effector velocity and hence can be lower bounded as follows:

$$-\dot{p}^T(\beta\gamma\hat{Q}_d + \alpha Q_d)M_p\dot{p} - (\alpha e_p + \beta\bar{n}_d)^T Z(q,\dot{q})\dot{p} + \xi_p(\|\dot{p}\|)(\alpha Q_{cd}\Delta p_t + \beta\bar{n}_{cd})^T\dot{p}_t \geq -\{(\beta\gamma+\alpha)\lambda_M + (c+\tilde{\xi})\|\alpha Q_{cd}\Delta p_t + \beta\bar{n}_{cd}\|\}\|\dot{p}\|^2. \quad (26)$$

Moreover, using (15), (16) and (9) we can lower bound the terms of the third and fourth line of (20), respectively,

$$\alpha\beta\gamma\,\dot{p}^T M_p\bar{Q}_d\Delta p - \alpha^2 k_v e_p^T\bar{Q}_d\Delta p + \alpha f_d\bar{n}_d^T\bar{Q}_d\Delta p - \alpha k_v\dot{p}^T\bar{Q}_d\Delta p \geq -[\alpha(\beta\gamma\lambda_M + k_v)\|\dot{p}\| + \alpha^2 k_v\|Q_{cd}\Delta p_t\| + \alpha f_d\|\bar{n}_{cd}\|]\|\bar{n}_{cd}\|\|\Delta p_t\| \quad (27)$$

$$(\alpha f e_p + \beta f\bar{n}_d + f_d\dot{p})^T\delta n \geq -c_n(\alpha f_M\|Q_{cd}\Delta p_t\| + \beta f_M\|\bar{n}_{cd}\| + f_d\|\dot{p}\|)\|Q_{cd}\Delta p_t\| \quad (28)$$

$$(\beta k_v + f_d)\bar{n}_d^T\hat{n}_d\hat{n}_d^T\dot{p} + \beta\bar{n}_d^T n_d\Delta f \geq -\frac{1}{2}\{(\beta k_v + f_d)\|\dot{p}\| + |\Delta f|\}\|\bar{n}_{cd}\|^2 \quad (29)$$

where f_M is the maximum value of the exerted force. Substituting (26)–(29) and using $\xi_p,\ \xi_\phi \geq 0$ into (20) yields:

$$W \geq \left\{\frac{k_v}{8} - \beta\gamma\lambda_M - (c+\tilde{\xi})\|\alpha Q_{cd}\Delta p_t + \beta\bar{n}_{cd}\|\right\}\|\dot{p}\|^2 + \left(\frac{k_v}{8} - \alpha\lambda_M\right)\|\dot{p}\|^2 + \alpha\left(\frac{\alpha k_v}{4} - c_n f_M\right)\|Q_{cd}\Delta p_t\|^2 + \frac{\beta}{2}(f_d - |\Delta f|)\|\bar{n}_{cd}\|^2 + \frac{1}{4}z_1^T A_1 z_1 + \frac{1}{4}z_1^T B_1 z_1 + \frac{1}{4}z_1^T C_1 z_1 + \frac{1}{4}z_2^T A_2 z_2 + \frac{1}{4}z_3^T A_3 z_3 + \frac{1}{4}z_3^T B_3 z_3, \quad (30)$$

where $z_1 = [\|\dot{p}\|\ \ \|\bar{n}_{cd}\|]^T$, $z_2 = [\|\dot{p}\|\ \ \|Q_{cd}\Delta p_t\|]^T$, $z_3 = [\|Q_{cd}\Delta p_t\|\ \ \|\bar{n}_{cd}\|]^T$ and

$$A_1 = \begin{bmatrix} k_v & -(\beta k_v + f_d)\|\bar{n}_{cd}\| \\ -(\beta k_v + f_d)\|\bar{n}_{cd}\| & \frac{\beta f_d}{2} \end{bmatrix},$$

$$B_1 = \begin{bmatrix} k_v & -2\alpha k_v\|\Delta p_t\| \\ -2\alpha k_v\|\Delta p_t\| & \frac{\beta f_d}{2} - 4\alpha f_d\|\Delta p_t\| \end{bmatrix},$$

$$C_1 = \begin{bmatrix} \frac{k_v}{2} & -2\alpha\beta\gamma\lambda_M\|\Delta p_t\| \\ -2\alpha\beta\gamma\lambda_M\|\Delta p_t\| & \frac{\beta f_d}{2} \end{bmatrix},$$

$$A_2 = \begin{bmatrix} \frac{k_v}{2} & -2(\alpha\beta\gamma\lambda_M + c_n f_d) \\ -2(\alpha\beta\gamma\lambda_M + c_n f_d) & \alpha^2 k_v \end{bmatrix},$$

$$A_3 = \begin{bmatrix} \alpha^2 k_v & -2\alpha^2 k_v\|\Delta p_t\| \\ -2\alpha^2 k_v\|\Delta p_t\| & \frac{\beta f_d}{4} \end{bmatrix},$$

$$B_3 = \begin{bmatrix} \alpha^2 k_v & -2c_n\beta f_M \\ -2c_n\beta f_M & \frac{\beta f_d}{4} \end{bmatrix}.$$

The following conditions guarantee a positive sign for each of the first four terms of (30), respectively,

$$\|\alpha Q_c\Delta p_t + \beta\bar{n}_{cd}\| < \frac{k_v - 8\beta\gamma\lambda_M}{8(c+\tilde{\xi})} \quad \text{with } k_v > 8\beta\gamma\lambda_M \quad (31)$$

$$k_v > 8\alpha\lambda_M \quad (32)$$

$$k_v > \frac{4c_n f_M}{\alpha} \quad (33)$$

$$|\Delta f| < f_d. \quad (34)$$

The determinants of the matrices A_i, B_i, C_i are non-negative if

$$\|\bar{n}_{cd}\| < \frac{\sqrt{2\beta k_v f_d}}{2(\beta k_v + f_d)} \quad (35)$$

$$\|\Delta p_t\| \leq \min\left\{\frac{f_d}{2\alpha k_v}\left(\sqrt{1 + \frac{\beta k_v}{2f_d}} - 1\right), \frac{\beta}{8\alpha}\right\} \quad (36)$$

$$\|\Delta p_t\| \leq \frac{1}{4\alpha\gamma\lambda_M}\sqrt{\frac{k_v f_d}{\beta}} \quad (37)$$

$$k_v > 2\sqrt{2}\left(\beta\gamma\lambda_M + \frac{c_n f_d}{\alpha}\right) \quad (38)$$

$$\|\Delta p_t\| \leq \frac{1}{4\alpha}\sqrt{\frac{\beta f_d}{k_v}} \quad (39)$$

$$k_v > \frac{16c_n^2 f_M^2\beta}{\alpha^2 f_d}. \quad (40)$$

Notice that condition (34) implies a maximum exerted force $f_M = 2f_d$. Hence, function W is positive definite with respect to $\dot{p}$, $\bar{n}_{cd}$ and $Q_{cd}\Delta p_t$ if the system solution remains within a region defined by the intersection of (31), (34)–(37) and (39), and k_v satisfies conditions (32), (33), (38) and (40) that are more restrictive than (22). □

The above stability conditions can be combined to a gain condition and to three conditions regarding the allowable uncertainty and the allowable position and force errors that define a stability region. In order to guarantee that the solution

https://doi.org/10.1017/S026357470800430X Published online by Cambridge University Press

will be restricted in the stability region, we must show that an estimate of the domain of attraction is contained within it.

In order to allow a maximum possible uncertainty we set $\beta = \frac{f_d}{k_v}$ and hence (35) becomes:

$$\|\bar{n}_{cd}\| < \frac{\sqrt{2}}{4}. \tag{41}$$

This region corresponds to a maximum estimation error angle of $\varphi_M \simeq 20^\circ$. For this choice of β we specify the Δp_t region from (36) and (39) and satisfy (37) with an appropriate choice of damping gain:

$$\|\Delta p_t\| \le r_0 \quad \text{where} \quad r_0 = \frac{f_d}{\alpha k_v}\frac{\sqrt{3/2}-1}{2} \tag{42}$$

$$k_v > \sqrt{4\gamma\lambda_M f_d \frac{\sqrt{3/2}-1}{2}}. \tag{43}$$

Furthermore, using (41), (42) and $\|Q_{cd}\Delta p_t\| \le \|\Delta p_t\|$, (31) is satisfied, by the following choice of k_v:

$$k_v > \sqrt{2f_d\left[(3\sqrt{2}-2)(c+\tilde{\xi}) + 4\gamma\lambda_M\right]} \tag{44}$$

that is more restrictive than (22), (43). Conditions (33), (38) and (40) involving the curvature parameter c_n can be satisfied by the following choice of k_v ($f_M = 2f_d$):

$$k_v > \max\left\{\frac{8c_n f_d}{\alpha}, 2\sqrt{2}\left(\beta\gamma\lambda_M + \frac{c_n f_d}{\alpha}\right)\right\}. \tag{45}$$

The aforementioned condition can be combined with (32), (44) into:

$$k_v > \max\left\{\sqrt{2f_d\left[(3\sqrt{2}-2)(c+\tilde{\xi}) + 4\gamma\lambda_M\right]}, 8\alpha\lambda_M, \frac{8c_n f_d}{\alpha}, 2\sqrt{2}\left(\beta\gamma\lambda_M + \frac{c_n f_d}{\alpha}\right)\right\}. \tag{46}$$

Therefore, for the case of maximum allowable uncertainty the stability region is defined by (34), (41) and (42) and the gain condition is (46).

From (42) it is obvious that the position error region becomes bigger if we choose small values for α, and big values for the desired force f_d. Moreover, k_v should be close to its lower bound given by (46), so that big position errors are allowed (42). Furthermore, region (34) practically means that the contact is maintained corresponding to a potential energy $I(\delta x)$ less than an upper bound I_U ($I(\delta x) < I_U$) as well as that the force response has less than 100% overshoot ($f < 2f_d$) corresponding to $I(\delta x) < I_O$ (fig. 2).

Proposition 3. *An estimate of the domain of attraction that is contained in the stability region defined by (34), (41) and (42) is given by:*

$$\Omega_\sigma = \left\{\dot{p}_t, \omega_t, \bar{p}_t, e_\phi, \bar{n}_{cd} \in \Re^3 : \; V(\dot{p}, \delta x, Q_{cd}\Delta p_t, e_\phi, \bar{n}_{cd}) < \sigma\right\},$$

where $\sigma = \min(\sigma_0, \sigma_1, \sigma_2)$ *with*

$$\sigma_0 = \min(I_U, I_O)$$

$$\sigma_1 = \frac{f_d}{8k_v^2\gamma}\left(k_v^2 - \gamma f_d \lambda_M\right)$$

$$\sigma_2 = \frac{\kappa_d\alpha\left(k_v - 2\alpha\lambda_M\right)(r_0 - |d| - r_{cd})^2}{2\alpha(k_v - 2\alpha\lambda_M) + (1+c_p)^2\kappa_d}$$

provided that $r_0 > |d| + r_{cd}$.

Proof: Substituting (7) in (8) we find

$$\Delta p_t = Q_{cd}\Delta p_t - n_{cd}(\cos\vartheta r_c + d) + n_{cd}n_{cd}^T(p_c - p_{cd}).$$

Using (10) in the above expression, we get

$$\|\Delta p_t\| \le (1+c_p)\|Q_{cd}\Delta p_t\| + r_c + |d|,$$

and hence (42) is satisfied if

$$|\delta x| + (1+c_p)\|Q_{cd}\Delta p_t\| < r_0 - r_{cd} - |d|. \tag{47}$$

If $|d| + r_{cd} < r_0$, (47) defines a region for δx, $Q_{cd}\Delta p_t$. Using (5) in (25) we get $V \ge \frac{1}{2}y^T P y$ with $y = [\,|\delta x| \;\; \|Q_{cd}\Delta p_t\|\,]^T$ and $P = \text{diag}\,[\kappa_d, 2\alpha(k_v - 2\alpha\lambda_M)]$. We can also find a positive constant[13]

$$\sigma_2 = \frac{(r_0 - r_{cd} - |d|)^2}{2b^T P^{-1} b},$$

where $b = [1 \;\; 1+c_p]^T$ so that (47) is replaced by $V < \sigma_2$. Furthermore, using (25), conditions (34), (41) can be replaced by $V < \sigma_0$ and $V < \sigma_1$, respectively. Since, V is positive definite, the choice $\sigma = \min(\sigma_0, \sigma_1, \sigma_2)$ completes the proof. □

Theorem. *There exists a domain of attraction* $\Omega_\sigma = \{\dot{p}_t, \omega_t, \bar{p}_t, e_\phi, \bar{n}_{cd} \in \Re^3 : \; V(\dot{p}, \delta x, Q_{cd}\Delta p_t, e_\phi, \bar{n}_{cd}) < \sigma\}$ *such that the estimator (12) used within the input control law (11) achieves force regulation* ($f \to f_d$)*, minimization of the position error* ($Q_{cd}\Delta p_t \to 0$) *and identification of the normal direction at the desired position* ($\hat{n}_{cd} \to n_{cd}$)*, provided that* $r_0 > |d| + r_{cd}$ *and* k_v *is chosen to satisfy condition (46).*

Proof: Starting within Ω_σ defined in Proposition 3, implies $V(t) \le V(0) < \sigma$ and hence $(\dot{p},\ \Delta f,\ Q_{cd}\Delta p_t,\ \bar{n}_{cd}) \in \mathcal{L}_\infty$. By virtue of $\frac{dV}{dt} + W = 0$ and Propositions 2–3, we get $(\dot{p},\ \bar{n}_{cd},\ Q_{cd}\Delta p_t) \in \mathcal{L}_2$. Equations (8), (17) further imply $\Delta p, \ddot{p} \in \mathcal{L}_\infty$ while Eq. (12) implies the boundedness of $\dot{\bar{n}}_{cd} = -\dot{\hat{n}}_{cd}$. Hence, $\dot{p}$, $\bar{n}_{cd}$ and $Q_{cd}\Delta p_t$ are uniformly continuous. Then, it follows from Desoer and Vidyasagar (1975)[14] that $\dot{p} \to 0, \bar{n}_{cd} \to 0 \Rightarrow \hat{n}_{cd} \to n_{cd}$, $Q_{cd}\Delta p_t \to 0$ and consequently $n_c \to n_{cd}$. Substituting in (17) we get $[n_{cd}^T\Delta f \;\; k_\phi e_\phi^T] = 0$ and hence from LaSalle's invariance theorem we get $f \to f_d$ and in turn $\phi_t \to \phi_{td}$. □

In a practical situation control gains k_v and γ should be chosen so as to satisfy (43) and α should be chosen small enough to satisfy (42) and $|d| + r_{cd} < r_0$. The estimate of

https://doi.org/10.1017/S026357470800430X Published online by Cambridge University Press

the domain of attraction given in Proposition 3 is based on strict sufficient conditions for the positiveness of W and it is therefore a conservative one. It is anticipated that the actual domain of attraction will be much greater, as it is also indicated in the simulation example of the following section.

Remark: Notice that we have proved the convergence of $\dot{p}$ to zero that corresponds to zero joint velocities in the non-redundant case away from singular positions. In the case of redundant robotic fingers the stability and convergence analysis is more involved because it additionally requires the proof of the exponential convergence of the joint velocities to zero that would guarantee that the system will not exhibit any internal motion. Simulation runs of redundant cases have shown target achievement.

5. Simulation Results

A 3-dof planar robotic finger with revolute joints is simulated using link lengths $l_1 = l_2 = 0.3$ m, $l_3 = 0.12$ m masses $m_1 = m_2 = 0.32$ kg, $m_3 = 0.16$ kg, inertias $I_i = \frac{m_i l_i^2}{12}$ and fingertip radius $r = 0.04$. The surface is modeled by a circle with center $(0.3980, 0.2897)$ and radius 0.2388 m. The normal force magnitude and the friction used in the simulation are $f = k_s \Delta x^2$ where k_s =250,000 and $F_s = 7.5 Q \text{diag}\,[|\dot{p}|]\,\dot{p}$. The contact point initial position is $p_c(0) = [\,0.1762 \;\; 0.2010\,]^T$ (m), the initial rigid tip orientation is -30° and the initial normal contact force is $f(0) = 23$ N. The control purpose is to exert a desired force of $f_d = 32$ N and to move to the point p_{td} without loosing contact while keeping the initial orientation. We set the initial estimate of the desired normal vector $\hat{n}_{cd}(0)$ equal to the initial normal vector. This implies a flat surface estimate; however, as the surface is curved, there is an estimate error that depends on the surface curvature and the distance the robot tip is required to cover.

The following choice of initial position error, estimation error and controller gains is a starting point within the region of attraction: $\|\Delta p_t(0)\| = 0.0347$ m, $\varphi(0) = -1.8^\circ$ and $\alpha = 0.6$, $\gamma = 30$, $k_v = 1600$, $k_\phi = 400$. Notice, that in order to start within the region of attraction the initial position error and estimation error are small and the controller gains α, k_v are chosen so that the system is slow. In fact, position error converges in more than 10 s. However, as the region of attraction estimate is very conservative the control target can be achieved for bigger position and estimation angle errors and a much faster response is possible with the appropriate choice of control gains. In fact we consider the case of position target $p_{td} = [\,0.18 \;\; 0.3\,]^T$ (m) that corresponds to a much bigger initial position error $\|\Delta p_t(0)\| = 0.1148$ m and estimation error of $\varphi(0) = -24.5^\circ$. Control gains α, k_v are set equal to 12 and 85 respectively while the rest of the gains remain the same. In Fig. 5 we depict the initial and the final (desired) position of the finger. Simulation results depicted in Figs. 6–8 show that the state converges to the desired values. In particular, force (Fig. 6), position error (Fig. 7) and the angle between the estimated and the actual normal vector at the desired position (Fig. 8) converge in less than 1 s. These results show that the control target can be achieved in a state region much greater than the one provided by the theoretical analysis.

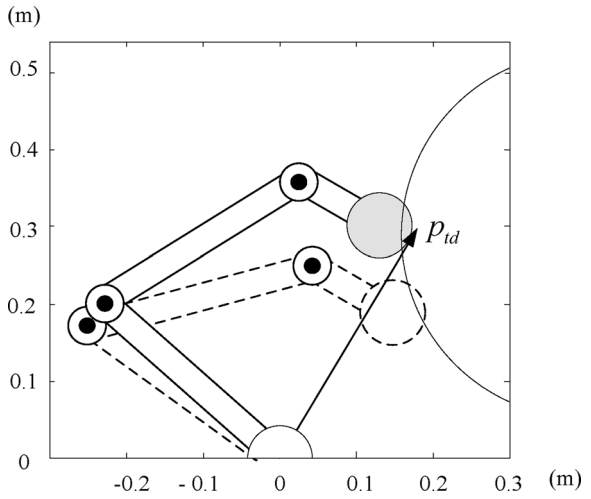


Fig. 5. Robotic finger of 3 dof in contact with a curved surface: initial position (dashed line) and final position (solid line).

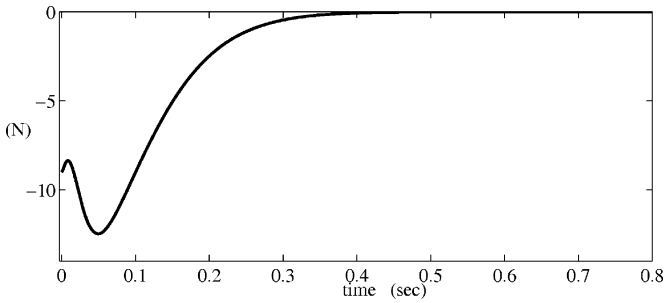


Fig. 6. Force error.

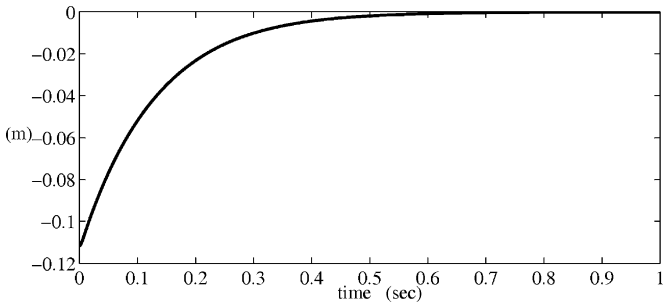


Fig. 7. Position error along the surface tangent.

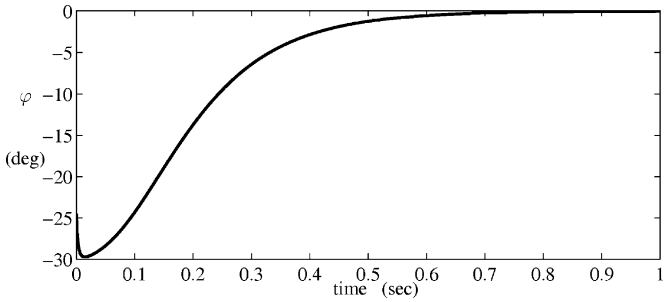


Fig. 8. Angle between the estimated and the actual normal vector at the desired position.

https://doi.org/10.1017/S026357470800430X Published online by Cambridge University Press

6. Conclusion

A simple controller with motion variable feedback is proposed that guarantees force/position regulation for the case of compliant contact with an unknown curved surface. The force and position control actions are separated into estimated complementary subspaces that are on-line tuned through a novel adaptive law to the actual subspaces at the desired point. The local asymptotic stability of the desired state equilibrium is proved and an estimate of the region of attraction is given. The simulation example illustrates the controller's performance, showing that it can be successfully used even if the system initial state is outside the estimated region of attraction.

References

1. M. H. Raibert and J. J. Craig, "Hybrid position/force control of manipulators," *ASME J. Syst. Meas. Control* **103**, 126–133 (1981).
2. S. Chiaverini and L. Sciavicco, "Force/position regulation of compliant robot manipulators," *IEEE Trans. Robot. Autom.* **9**(4), 361–373 (1993).
3. C. C. Cheah, S. Kawamura and S. Arimoto, "Stability of hybrid position and force control for robotic kinematics and dynamics uncertainties," *Automatica* **39**, 847–855 (2003).
4. Y. Zhao and C. C. Cheah, "Hybrid Vision-force Control for Robot with Uncertainties," *Proceedings of the IEEE 2004 International Conference on Robotics and Automation*, New Orleans, (2004) pp. 261–266.
5. T. Yoshikawa and A. Sudou, "Dynamic hybrid position/force control of robot manipulators—On-line estimation of unknown constraint," *IEEE Trans. Robot. Autom.* **9**(2), 220–226 (1993).
6. D. Xiao, B. Ghosh, N. Xi and T. Tarn, "Sensor-based hybrid position/force control of a robot manipulator in an uncalibrated environment," *IEEE Trans. Control Syst. Technol.* **8**(4), 635–645 (2000).
7. M. Namvar and F. Aghili, "Adaptive force-motion control of coordinated robot interacting with geometrically unknown environments," *IEEE Trans. Robot. Autom.* **21**(4), 678–694 (2005).
8. M.Namvar and F. Aghili, "Adaptive Force Control of Robots in Presence of Uncertainty in Environment," *Proceedings of the 2006 American Control Conference*, Minneaopolis, (Jun. 2006) pp. 3253–3258.
9. T. Olsson, J. Bengtsson, R. Johansson and H. Malm, "Force Control and Visual Servoing using Planar Surface Identification," *Proceedings of the IEEE 2002 International Conference on Robotics and Automation*, Washington DC, (May 2002) pp. 4211–4215.
10. Z. Doulgeri and Y. Karayiannidis, "Performance analysis of a Soft Tip Robotic Finger Controlled by a Parallel Force/Position Regulator under Kinematic ncertainties," *IET Control Theory and Applications* **1**(1), pp. 273–280, 2007.
11. Z. Doulgeri and Y. Karayiannidis, "Force position control for a robot finger with a soft tip and kinematic uncertainties," *Robot. Auton. Syst.* **55**(4), 328–336 (2007).
12. Y. Karayiannidis and Z. Doulgeri, "An Adaptive Law for Slope Identification and Force Position Regulation using Motion Variables," *Proceedings of the IEEE 2006 International Conference on Robotics and Automation*, Orlando, (May 2006) pp. 3538–3543.
13. H. Khalil, *Nonlinear Systems*, 3rd ed. (New Jersey, Prentice Hall, 2002).
14. C. A. Desoer and M. Vidyasagar, *Feedback Systems: input-output properties*, (Academic Press, New York, 1975).

https://doi.org/10.1017/S026357470800430X Published online by Cambridge University Press